

Optimisation of the operating voltage of a multilayer uniaxial dielectric elastomer generator

Wojciech Sikora^{1*} , Krzysztof Michalczyk¹ 

¹ Department of Machine Design and Maintenance, Faculty of Mechanical Engineering and Robotics, AGH University of Krakow, al. A. Mickiewicza 30, 30-059 Krakow, Poland

* Corresponding author's e-mail: wosikora@agh.edu.pl

ABSTRACT

The optimum operating parameters for dielectric elastomer generator (DEG) systems, in the sense of the global optimum, refer to their maximum performance in terms of elastomer tensile strength, breakdown voltage value etc. In practice, operating a DEG close to the limit of its strength will involve a limitation of its durability, as DEGs can also suffer fatigue damage. Deviation from the optimum operating parameters, either for reasons of increasing their durability and reliability or simply because of practical limitations in a given application, makes it necessary to search for local optimum operating points. The aim of this study was to analytically determine the optimum working point of a DEG generator operating in a rectangular cycle (constant charge, constant voltage) by the value of the voltage difference between the upper and lower sources. On the basis of capacitance measurements on two generators with two and three active layers (electrodes) operating under uniaxial tensile loading, the theoretical values of the optimal voltage difference ΔU were calculated. The results were then verified experimentally. The empirical values were found to be in agreement with the theory and showed that it is possible to predict the performance of a DEG accurately by knowing the variations in its electrical capacitance.

Keywords: DEG, dielectric elastomer generator, energy harvesting, optimization, uniaxial.

INTRODUCTION

Systems for converting mechanical energy into electrical energy can utilize various phenomena like piezoelectricity [1] or electromagnetic induction [2]. Those based on the flexible capacitor concept, are referred to in the literature by the abbreviation DEG. They have two distinctive features. The first is the relatively low stiffness that causes DEGs to operate in the high relative deformation range at low loading forces. This is due to the use of elastomeric materials as the flexible dielectric of the capacitor. This stands in opposition to the most popular harvester systems that use piezoelectrics, ceramic or macro fibre composite (MFC) [3], which are characterised by stiffnesses several orders of magnitude higher than typical elastomers. The second feature is related to the fact that DEGs require power supply to operate. Although this is initially counterintuitive

given the power-generating function, it is related to the specific working characteristics of DEGs. Their task is to raise the potential of the electrical charge already stored in them, which must first be drawn from a voltage source.

Due to the low values of the relative electrical permeability [4] of most elastomeric materials used for DEG membranes, in order to obtain useful amounts of energy, the generators must have a large working area or operate at high voltages on the order of kilovolts [5]. This causes the search for methods to optimise the structural and operating parameters of DEGs [6, 7, 8, 9, 10], also in the area of material selection [11, 12]. Much of this work is concerned with the functioning of DEGs near their limits due to mechanical strength [13], dielectric electrical breakthrough [14, 15] or electromechanical stability. From a theoretical point of view, this is the right direction, but in practice this approach may limit the

durability of generators due to ignoring fatigue phenomena [16]. Although there is currently a lack of commercial products using DEGs, there are papers published describing prototype generators for wave power generation [17–19] based on the concept of flexible capacitors and DEGs, where the issue of durability will determine the economic viability of such projects. Nevertheless, it must be assumed that, when operating under real-world conditions, DEG systems will operate below their optimum capacity for safety and durability reasons, as is the case in almost all engineering designs.

It therefore seems reasonable to develop methods for determining ‘‘local’’ optimal parameters for the dictated conditions associated with a particular application. For example, the electrical capacitance of a DEG may be limited by the available deformation space or load amplitude. Also, the supply voltage may be determined by other factors and impossible to change.

This paper presents a methodology for determining the optimum value of the differential voltage ΔU leading to the maximum amount of energy in the DEG for a given variation of capacitance and supply voltage U_1 . The theoretical calculations were verified in the experimental part with measurements on physical specimens of multilayer DEGs.

DEG WORKING CYCLE AND OPTIMAL VOLTAGE

A generator that uses a flexible membrane acting as a dielectric is in fact a deformable elastic capacitor. Changes in its dimensions during physical deformation affect the electrical capacitance which can be used to increase the potential of the electrical charge that is stored in it. A detailed description of the functioning of a DEG with a structure identical to the one described in this paper can be found in [20]. A flexible capacitor by itself cannot be used to generate an electrical charge as is the case with piezoelectric materials. Instead, it is used to increase the potential of the electric charge taken in the ‘charge’ phase from a source with a voltage U_1 and transferred in the ‘discharge’ phase to a source with a higher voltage U_2 . Between the charging and discharging phases, stretching and relaxation of the dielectric membrane takes place, during which the capacitance of the capacitor increases and

decreases respectively. The charge accumulated during charging at the highest capacitance is later, during relaxation, compacted when, with a constant amount of electrical charge and decreasing capacitance, its potential increases. The elastic energy stored in the stretched membrane is then converted into electrical energy accumulated in the electrical charge with increased potential. The theoretical loop of the duty cycle in the form of a voltage vs charge plot has a rectangular shape as shown in Figure 1.

The duty cycle used is called the rectangular cycle [21] or constant-charge (CC) or constant-charge constant-voltage (CCCV) [22]. It is not the best cycle in terms of the amount of energy produced. The better one is the so-called triangular cycle [23]. However, the rectangular cycle has the advantage of using a simple harvesting circuit and of not having to use switches. In the triangular cycle switches have to be open and closed in synchronisation with certain DEG deformation phases. The rectangular cycle could also be used without additional configuration for non-harmonic or stochastic loads.

In the present work, the values describing the operating parameters of the DEG in the state of maximum stretch, i.e. the highest capacitance C_1 , the amount of electrical charge Q_1 and the lower voltage value U_1 , are denoted by index 1. Similarly, for the state of minimum length of the DEG, index 2 is used. Thus, the amounts of charge accumulated at these two characteristic operating points of the generator are described by the relations:

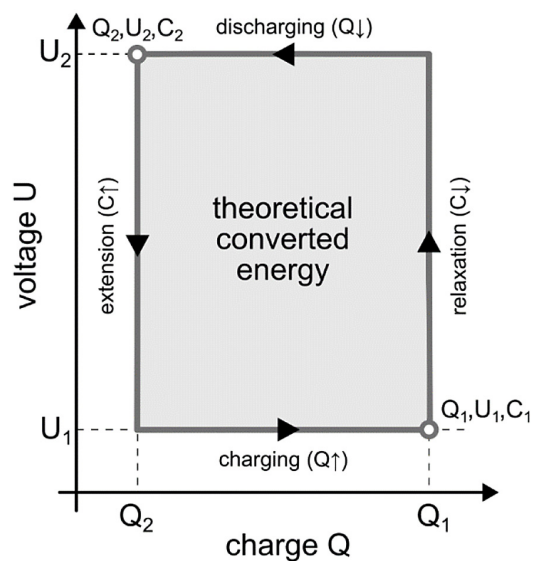


Figure 1. Ideal working cycle of a DEG with no leaks in the harvesting circuit

$$Q_1 = C_1 \cdot U_1, Q_2 = C_2 \cdot U_2 \quad (1)$$

The amount of charge that should flow theoretically out from the capacitor at the transition from point 1→2 amounts to:

$$\Delta Q = Q_1 - Q_2 = C_1 \cdot U_1 - C_2 \cdot U_2 \quad (2)$$

Assuming that the capacitance changes will be harmonic, they will be described by the mean value C_m and the peak-to-peak amplitude ΔC :

$$C_m = \frac{C_1 + C_2}{2}, \Delta C = C_1 - C_2 \quad (3)$$

The amount of energy that is associated with the outflow of a ΔQ -value charge at a constant value of voltage U_2 , which was previously raised from voltage U_1 , can be calculated from the relationship:

$$\begin{aligned} \Delta E &= \Delta U \cdot \Delta Q = \\ &= \Delta U \cdot (\Delta C U_1 - C_m \Delta U + 0.5 \Delta C \Delta U) \end{aligned} \quad (4)$$

where: $\Delta U = U_2 - U_1$

The relationship (4) is shown as a contour plot (Fig. 2) for the values associated with the selected load variant of the 3-layer generator (deformation amplitude $A = 6$ mm, peak-to-peak 12 mm).

Analysing the relationship (4), it can be seen that the energy obtained can, theoretically, be negative due to the term $C_m \cdot \Delta U$ appearing there with a negative sign. In practice, this means that for certain combinations of values of the DEG operating parameters, the phenomenon of conversion of mechanical energy to electrical energy will not occur on a scale sufficient to allow charge flow to the source U_2 . In other words, the increase

in voltage across the flexible capacitor will not satisfy the condition $U_1 + \Delta U \geq U_2$. The limiting values of ΔU are indicated in Figure 2 by the red line labelled $\Delta E = 0$.

The amount of energy obtained in the Equation 4 depends on the square of the voltage difference ΔU , while the direct effect of the other operating parameters is linear. This suggests that it may be possible to indicate the optimum value of the ΔU . In Figure 2 for a given value of the lower voltage U_1 , it is possible to indicate such a value of ΔU that will provide the highest possible amount of generated energy. Figure 2 shows the line of the optimal amount of energy plotted on the basis of the following relationship:

$$\frac{\delta(\Delta E)}{\delta(\Delta U)} = 0 \rightarrow \Delta U_{opt} = \frac{\Delta C \cdot U_1}{2C_m - \Delta C} \quad (5)$$

Using knowledge of the parameters describing the capacitance of the DEG (C_m and ΔC) and with an assumed value of the supply voltage U_1 , using Equation 5 it is possible to determine the optimum value of the voltage increase ΔU that will provide the greatest amount of energy.

Capacitance measurement

Two DEG systems with identical dimensions (Fig. 4), but differing in the number of active layers, were tested. The area of the electrodes in the initial state is 1750 mm². The DEG used in the study consists of a series of dielectric layers made of VHB4910 material. These were formed from

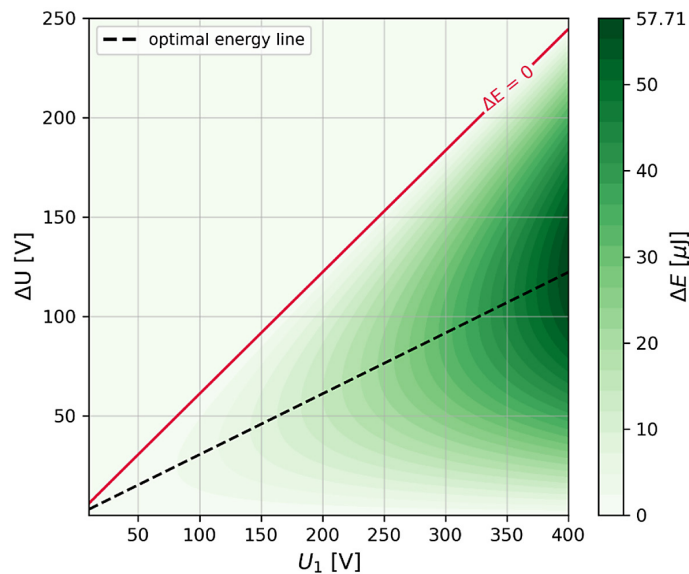


Figure 2. Amount of energy converted ΔE as a function of voltage U_1 and difference ΔU for a variable capacitance described by $C_m = 5.04$ nF and $\Delta C = 2.36$ nF

sheets of $30 \times 24 \times 1$ mm, which, when stretched to 105×120 mm, were transferred to a support frame (Fig. 3a) made using 3D printing [24, 25, 26]. The overhanging fragments were trimmed to frame size. Details of the assembly process can be found in [20]. The approximate thickness of the prestretched layer is 0.1 mm. Active layers were applied between dielectric layers, acting as capacitor electrodes. These layers are made of an electrically conductive grease (MG Chemicals 846-80G), so that they deform together with the flexible dielectric layers. The first DEG system contained 2 active layers and the second contained 3 layers. Adding more layers above the basic two, analogous to a plate capacitor, allows the capacitance of the generator to increase proportionally.

The DEG generator was mounted and stretched in a MTS Acumen 3 testing machine (Fig. 3b). The basic dimensions of the sample, including the surface area of the active layers, are given in Figure 4. The load was applied as a sinusoidal displacement with a frequency of 1 Hz, zero mean value and an amplitude equal to $A = (4, 6, 8)$ mm.

During deformation, changes in DEG capacitance were recorded using the current-voltage method (I-V method) described in [27]. It consists of measuring the amplitude and phase shift of a test voltage signal before and after a reference resistor connected in series prior to the capacitor being evaluated. The parameters of the sinusoidal test signal were: amplitude 10 V, mean value zero, frequency 100 Hz, reference resistance 470 k Ω . Direct measurements were made using a National Instruments (NI) USB-6003 measurement card and NI LabVIEW software. An example of the time series of capacitance change is shown in Figure 5 and the results of all measurements are included in Table 1.

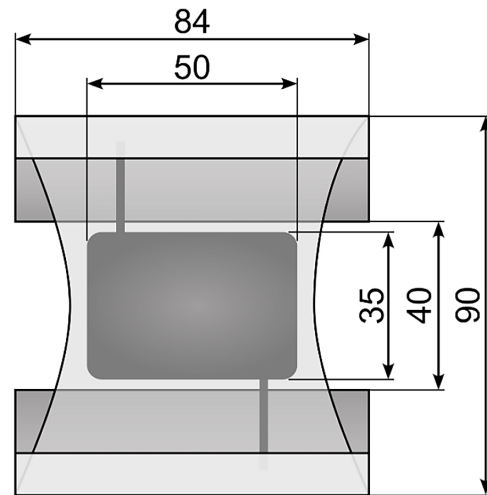


Figure 4. DEG dimensions in [mm]

ENERGY MEASUREMENTS

The conversion of mechanical energy into electrical energy using a flexible capacitor is only possible if the capacitor is connected to a dedicated electrical circuit. Its task is to ensure that the flow of electrical charge is properly directed during the cyclic stretching of the generator. The circuit used in this work (Fig. 6) is known in the literature [28]. The reference voltages U_1 and U_2 are provided by a source 1 and a charged capacitor 4, respectively. The diodes 2 and 3 act as check valves to ensure that the charge accumulated on the generator 5 does not flow back to the source 1 during DEG relaxation and that current does not flow from the voltage U_2 4 back to the source U_1 1. An additional capacitor 6 plugged in series after the DEG 5 is used to measure the charge that flows through the DEG during operation. The electrical system and its parameters are the same as those described in the earlier work [20].

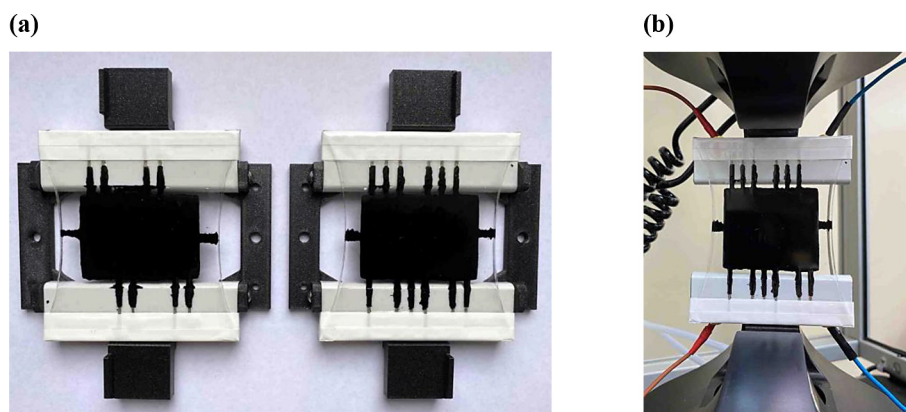


Figure 3. DEGs used in the study (a) (from left) 2- and 3-layer variant, (b) 3-layer sample mounted in the test machine

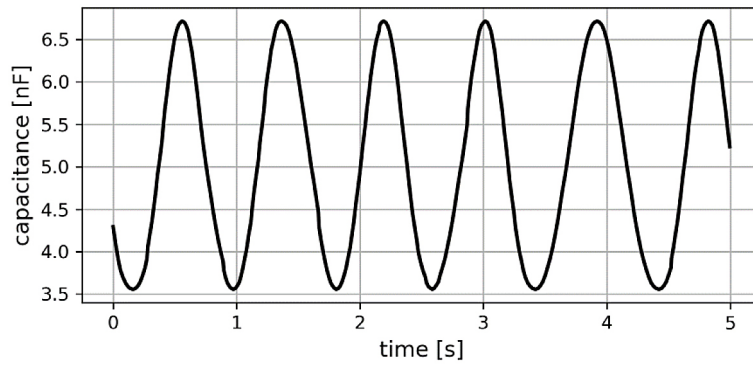


Figure 5. Recorded waveform of electrical capacitance variation of a 3-layer DEG under sinusoidal deflection amplitude $A = 8$ mm. Obtained values $C_m = 5.14$ nF, $\Delta C = 3.16$ nF

Table 1. Capacitance measurements

No	Active layers [-]	Amplitude A [mm]	ΔC [nF]	C_m [nF]
1	2	4	0.87	2.66
2	2	6	1.31	2.69
3	2	8	1.76	2.74
4	3	4	1.57	4.98
5	3	6	2.36	5.04
6	3	8	3.16	5.14

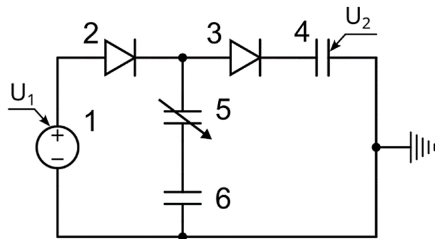


Figure 6. Electrical diagram of the harvester circuit: 1 – lower voltage source, 2, 3 – diodes controlling the charge flow, 4 – capacitor representing the upper voltage source, 5 – variable capacitor (DEG), 6 – capacitor for measuring the charge flowing through the DEG.

Due to the fact that the components building the electrical system from Figure 6 are not ideal, the actual work loop (Fig. 7a) of voltage vs charge deviates from that referenced earlier in Figure 1. Caused by the leaks in the circuit, primarily within the diodes, charge also flows through the DEG during periods when it is being stretched or relaxed and the charge should remain constant. In the Figure 1 this can be seen in the form of a deviation of the left and right edges of the loop, which should be perfectly vertical lines. Based on which phase of the cycle the leaks occur in, they can be divided into:

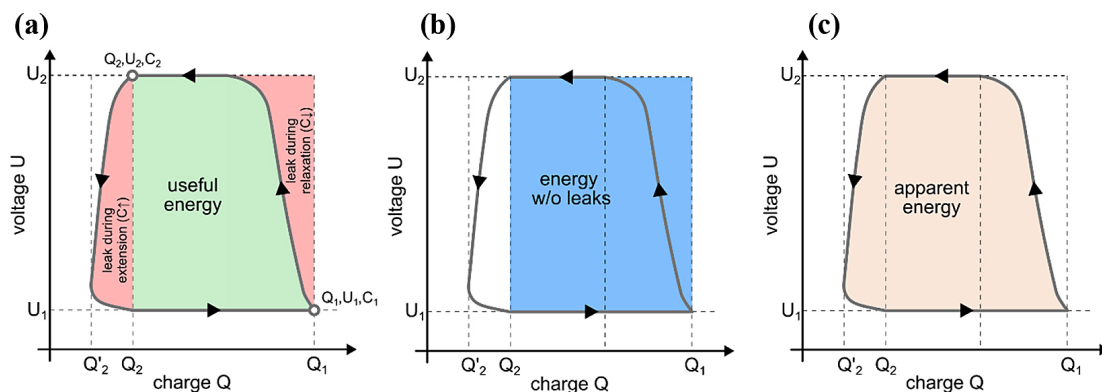


Figure 7. Estimation of the energy converted at DEG during the actual work cycle, (a) useful energy and leakage, (b) energy excluding losses, (c) apparent energy

- leakage during relaxation (transition from point 1 → 2) – in this case the energy is lost,
- leakage during stretching (2 → 1) – when the energy apparently increases.

The leakage of energy due to a decrease in charge level from Q_1 before it reaches the target voltage U_2 is easy to interpret. In contrast, in the second case, a leakage resulting in a decrease in charge from Q_2 to Q'_2 results in an increase of the operating loop and an apparent increase in the energy converted in the DEG. In a situation where the entire electrical system including the DEG would function without leakage, the amount of energy gained should correspond to the area marked in Fig. 7b. It should also coincide with the theoretical output calculated according to the Equation 4. The energy determined as the area of the whole loop (as in Fig. 7c) is an apparent energy, as it is too large in relation to the actual useful energy by the value of the energy associated with the leakage reducing the amount of charge from Q_2 to Q'_2 .

Five voltage levels $U_1 = 100, 150, 200, 250, 300$ V were selected for energy measurements and verification of analytical calculations. Then, for each level U_1 and the known capacitance C_m and ΔC the optimum value of the voltage difference ΔU was calculated according to the formula (5). This gave a total, for the two generators considered, 2- and 3-layer, and three load amplitudes, of $5 \cdot 2 \cdot 3 = 30$ series of measurements. In the vicinity of the theoretical value of the ΔU_{opt} five closely spaced values of the ΔU voltages were each assumed, so that an empirical optimum value could be determined,

resulting in $30 \cdot 5 = 150$ of direct measurements. Each of these measurements consisted of the recorded time series of the voltage on the DEG (Fig. 8a) and the charge flowing through the DEG (Fig. 8b). By compiling these data in the form of a charge vs voltage plot (Fig. 8c), an empirical operating loop was obtained. From its course, an estimate was then made of the converted useful energy ΔE (like in Fig. 7a) and energy with correction for leakage (similarly like in Fig. 7b). Point 2 (with reference to the one in Fig. 7a), which is needed to isolate losses during DEG stretching, was established as the inflection point of the generator working loop curve. This inflection takes place between the horizontal section at voltage U_2 and the voltage drop section $U_2 \rightarrow U_1$.

As described earlier, for each of the 30 measurement cases, five ΔU values were selected close to the expected optimal value determined analytically. For each of these five measurements, the energy value was determined and the resulting points were approximated by a standard quadratic function. The extrema of this function was then calculated and the corresponding ΔU and ΔE values were treated as the result in the given measurement case. Figure 9 shows an example of how, based on the experimental measurements, the optimum point was determined.

RESULTS

A summary of the energy measurement results at the optimum operating point of the DEG is shown in Figure 10. The results were divided

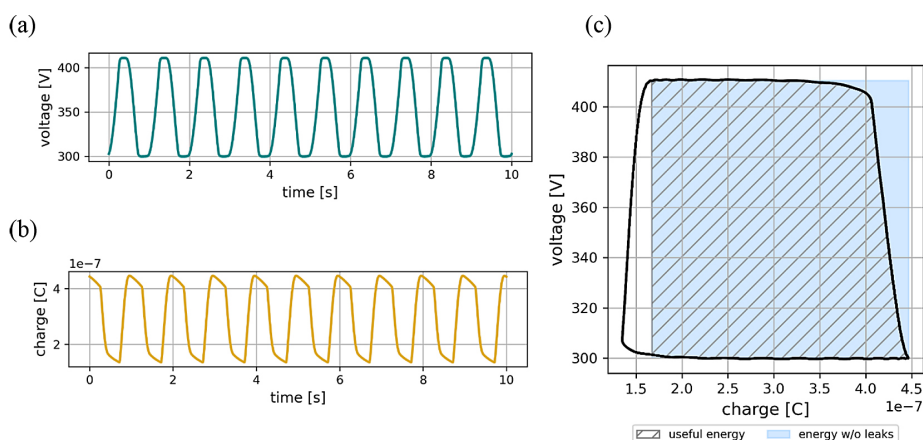


Figure 8. Example measurements required for energy assessment made of 3-layer sample, $A = 6$ mm, $U_1 = 300$ V and $U_2 = 410$ V: (a) DEG voltage vs time, (b) charge flowing through DEG over time, (c) voltage vs charge loop used to calculate amount of energy converted

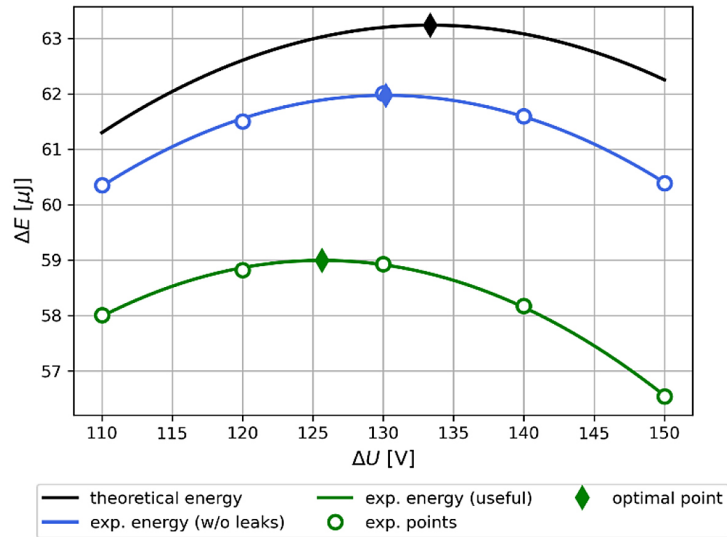
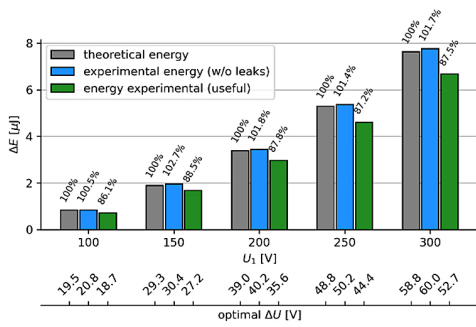
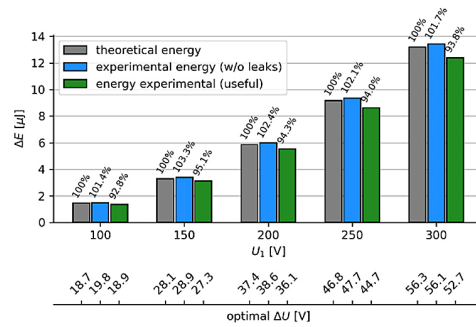


Figure 9. Comparison of the generated energy ΔE curves near the predicted optimum point for 3-layer DEG, $A = 8$ mm, $U_1 = 300$ V measurement

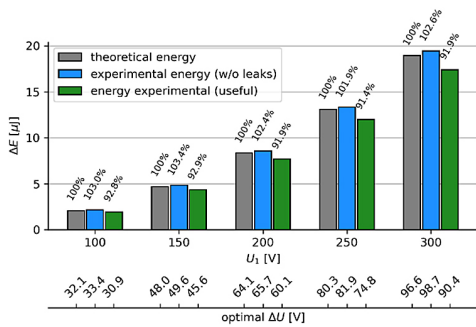
(a) 2-layers DEG, $A = 4$ mm



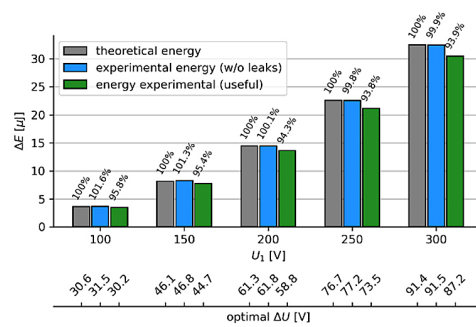
(b) 3-layers DEG, $A = 4$ mm



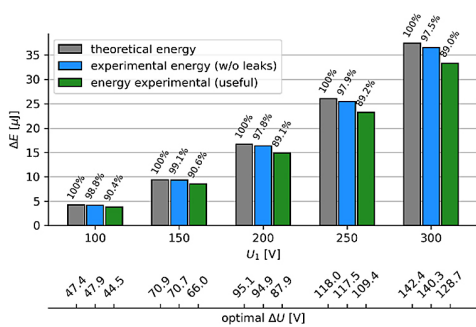
(c) 2-layers DEG, $A = 6$ mm



(d) 3-layers DEG, $A = 6$ mm



(e) 2-layers DEG, $A = 8$ mm



(f) 3-layers DEG, $A = 8$ mm

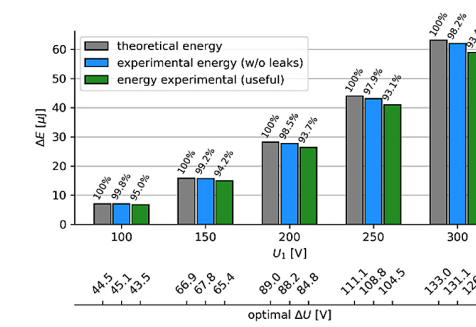


Figure 10. Comparison of ΔE energy obtained for the optimal ΔU value for specific U_1 voltages, number of DEG active layers and load amplitude

into six graphs according to the number of DEG active layers (2 and 3) and the load amplitude (4, 6 and 8 mm) set on the testing machine during the test. Each bar chart contains three series of data describing the energy obtained for a given base voltage U_1 and the optimum voltage difference ΔU given on the second, horizontal x -axis. The exact values have also been grouped in Table 2. The series sequentially correspond to:

- the theoretical energy, calculated from formula (4) and (5),
- measured energy with leakage compensation,
- measured effective energy.

Above each bar, for a given base voltage U_1 , its value related to the theoretical energy value is

given in percentage, which, constituting the base, equals 100 %.

The results from Figure 10 are also presented in comparison plots. The first of them (Fig. 11) compares the values of the optimum ΔU voltage difference calculated analytically and obtained by experimental measurements, for the energy measured without leakage and the actual effective energy. In an analogous manner, the results of ΔE energy are compared in Figure 12. In all cases shown in Figure 11 and 12, the Pearson correlation coefficient is equal to or greater than $R=0.999$. This indicates that the experimental results have a very high correlation with the theoretical values.

Table 2. Results of optimum energy and corresponding ΔU values for each sample and operating conditions

No	Active layers [-]	Amplitude A [mm]	U_1 [V]	theoretical		exper. w/o leaks		exper. useful	
				ΔU [V]	ΔE [μ J]	ΔU [V]	ΔE [μ J]	ΔU [V]	ΔE [μ J]
1	2	4	100	19.6	0.9	20.1	0.8	18.1	0.7
2	2	4	150	29.4	1.9	31.7	1.9	27.9	1.6
3	2	4	200	39.2	3.4	39.5	3.4	34.9	3.0
4	2	4	250	48.9	5.3	49.1	5.4	43.4	4.6
5	2	4	300	58.7	7.7	59.2	7.8	51.9	6.7
6	2	6	100	32.2	2.1	32.6	2.2	30.0	1.9
7	2	6	150	48.3	4.7	47.9	4.8	44.0	4.4
8	2	6	200	64.5	8.4	64.6	8.6	59.0	7.7
9	2	6	250	80.6	13.2	80.6	13.3	73.5	12.0
10	2	6	300	96.7	19.0	97.5	19.4	89.1	17.4
11	2	8	100	47.2	4.2	48.2	4.1	44.9	3.8
12	2	8	150	70.9	9.3	70.9	9.3	66.1	8.5
13	2	8	200	94.5	16.6	95.3	16.3	88.3	14.9
14	2	8	250	118.1	26.0	117.8	25.5	109.5	23.2
15	2	8	300	141.7	37.4	140.5	36.5	129.0	33.3
16	3	4	100	18.7	1.5	19.2	1.5	18.2	1.3
17	3	4	150	28.0	3.3	28.9	3.4	27.2	3.1
18	3	4	200	37.4	5.9	38.5	6.0	36.0	5.5
19	3	4	250	46.7	9.2	47.8	9.4	44.8	8.6
20	3	4	300	56.1	13.2	55.9	13.4	52.5	12.4
21	3	6	100	30.6	3.6	31.4	3.7	30.1	3.5
22	3	6	150	45.9	8.1	47.0	8.3	44.9	7.8
23	3	6	200	61.2	14.4	62.0	14.5	59.0	13.6
24	3	6	250	76.5	22.6	77.2	22.5	73.5	21.2
25	3	6	300	91.8	32.5	90.9	32.5	86.8	30.5
26	3	8	100	44.5	7.0	45.3	7.0	43.7	6.7
27	3	8	150	66.7	15.8	68.0	15.7	65.5	14.9
28	3	8	200	88.9	28.1	88.4	27.8	84.9	26.4
29	3	8	250	111.1	43.9	109.2	43.1	104.9	41.0
30	3	8	300	133.4	63.2	130.2	62.0	125.7	59.0

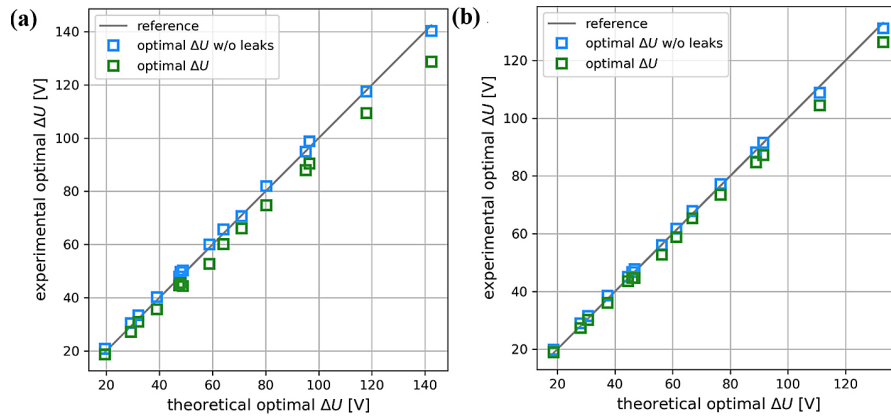


Figure 11. Comparative graph of the analytical estimation of the optimal ΔU values and the values obtained from the experiment for the (a) 2-layer, (b) 3-layer sample

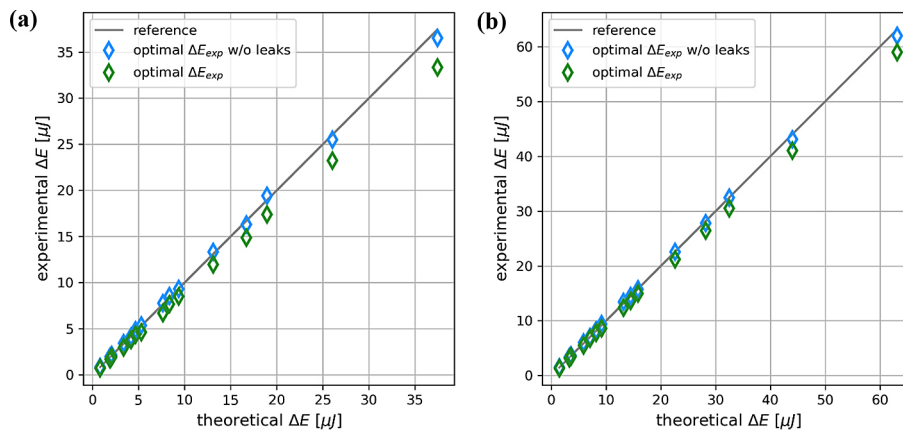


Figure 12. Comparative graph of the analytical estimation of the optimal ΔE values and the values obtained from the experiment for the (a) 2-layer, (b) 3-layer sample

DISCUSSION

The analysis started with a qualitative assessment of the correspondence of the empirical results ΔU_{opt} and ΔE with the theoretical values, which are shown in the comparison graphs Figure 11 and Figure 12. Three main phenomena can be observed on the basis of the distribution of the results:

- for both the 2-layer and the 3-layer sample, the points lie very close to the reference line, which means that the theoretical relationship is very well reproduced in practice; the points for the energy case excluding leakage coincide almost exactly with the reference line,
- the agreement is slightly better for the 3-layer sample.

These conclusions can be attributed to both the results of ΔU_{opt} and ΔE . The bar graphs showing the amount of energy generated (Fig. 10) display

the expected trend, related to the proportional influence of the voltage U_1 , the amplitude A and the number of active layers on the amount of energy generated, which is generally in line with that one resulting from Equation 4.

An observation that may come as a surprise is that in Figure 10, in some measurement cases, the measured energy with leakage compensation is higher than the value predicted by the theoretical formula. This situation occurs primarily for the 2-layer DEG, for displacement amplitudes $A = 4$ and 6 mm and for the 3-layer DEG and displacement amplitude $A = 4$ mm. As this is thus associated with smaller ranges of variation in electrical capacitance (ΔC) and thus the flow of less charge, the reason for obtaining such unphysical results can be attributed to:

- the inaccuracy of the capacitance measurement,
- inaccuracy of the energy measurement based on the empirical loop U vs Q .

The first factor could be related to the method of making the electrical capacitance measurement itself (the I-V method and the associated frequency of the test signal and the accuracy of the phase shift angle estimation). However, test measurements on commercial polymer capacitors described in [27] made with the measurement system also used in this work, suggest that the measurement error does not exceed 1%. Thus, it is more likely that any discrepancies between the measured and actual capacitance of the DEG during deformation are due to the specific functioning of the flexible capacitor. There is an electrically conductive grease between the elastic layers, which moves across the layers surfaces during cyclic stretching. This is not a fully repeatable process and this may account for the inaccurate estimation of the course of DEG capacitance changes.

The second factor is due to the fact that in a real working loop it is difficult to determine very accurately the value of the charge Q_2 , which determines the left boundary of the useful energy area (Fig. 7b). Even if the adopted value corresponds to the inflection point of the operating curve at point 2, the adopted value of Q_2 does not necessarily correspond exactly to the point at the bottom of the loop where the voltage reaches the lower value U_1 . Smaller amounts of charge flowing through the DEG also make interference and imperfections in the measurement system more apparent, making it more difficult to read the amount of energy from the DEG operating loop.

The operating voltage on the DEG can also affect changes in capacitance values under mechanical loading. It is conceivable that at high voltages, on the order of several kilovolts, electrostatic forces will significantly affect membrane deformation during stretching. The capacitance measurement in the paper was carried out with a test voltage signal of 10 V amplitude. Analysing the results, it seems that the fact of DEG operation at a voltage of 400 V did not cause significant discrepancies. However, it is not certain that at operating voltages higher by an order of magnitude such differences will not appear. One would then have to wonder whether carrying out capacitance measurements at higher test voltages would make up for these differences. Of course, this would entail modifying the measurement system so that it could operate at high voltages.

Despite the above-discussed aspects, the observed deviations of leakage-compensated energy values from the expected (theoretical) energy are

within the limit of less than $\pm 5\%$ and can be considered satisfactory.

A useful finding that also comes from Figure 10 is the effect of leakage on the amount of useful energy that can be extracted under the given conditions from the DEGs tested. Comparing individual measurement points, it is observed that leakage losses reach several percent, up to a maximum of 11% for a 2-layer DEG 2, $A = 8$ mm and base voltage $U_1 = 300$ V.

Although the results apply to DEG operation at the point of optimal ΔU , it can be assumed that no worse reproduction of the theoretical DEG performance will also be observed outside the voltage range studied in this paper.

CONCLUSIONS

The tests carried out showed that a DEG system operating in uniaxial stretching mode, with the design described in the paper, functions in good agreement with the theoretical relationships. The question the paper sought to answer was whether the physical phenomena, possible losses of mechanical and, above all, electrical nature, which occur in a real DEG, cause the theoretical dependencies describing charge flow in the energy conversion process not to be reflected in reality. This was especially true for the optimal voltage difference ΔU , which, according to theoretical predictions, was supposed to ensure that the maximum amount of energy was obtained for a given U_1 , C_m and ΔC .

The occurrence of the mentioned losses was observed in the course of the study. The theoretical results were compared with the empirical ones in the direct version and the version corrected for the occurrence of electric charge leakage. Comparison of the corrected results revealed discrepancies of a few percent, which were caused by imperfections in the measurement itself. From a practical point of view, however, they can be considered as in full agreement. On the other hand, the comparison of the actual results made it possible to observe that leaks in the DEG system in the studied range can reach up to 11%. Nevertheless, both the estimated optimal amount of energy ΔE as well as the voltage difference ΔU using theoretical formulas were sufficiently close to the actual experimental values. This means that for stationary DEG operating conditions and with a suitable harvester circuit, the modelling results sufficiently reflect the results of

the real system and can be used to design similar DEG systems. However, in order to carry out calculations, it is necessary to identify in advance the range of changes in DEG capacitance depending on its deformation.

In the future, similar tests would have to be performed for non-harmonic and stochastic loads, as DEG systems would eventually be expected to operate under excitation resulting from vibrations, sea waves or windmill rotation, which would involve irregular loading.

Acknowledgements

This work is financed by AGH University of Krakow, Faculty of Mechanical Engineering and Robotics, research program No. 16.16.130.942.

REFERENCES

- Ambrożkiewicz B., Czyż Z., Stączek P., Tiseira A., García-Tiscar J. Performance analysis of a piezoelectric energy harvesting system. *Advances in Science and Technology – Research Journal*. 2022 Nov 29;16(6):179–85. <https://doi.org/10.12913/22998624/156215>
- Kecik K. Experimental energy recovery from a backpack using various harvester concepts. *Advances in Science and Technology – Research Journal*. 2024 Apr 20;18(3):67–78. <https://doi.org/10.12913/22998624/185848>
- Grzybek D. Control system for multi-input and simple-output piezoelectric beam actuator based on macro fiber composite. *Energies*. 2022 Mar 10;15(6):2042. <https://doi.org/10.3390/en15062042>
- Vu-Cong T, Jean-Mistral C, Sylvestre A. Impact of the nature of the compliant electrodes on the dielectric constant of acrylic and silicone electroactive polymers. *Smart Materials and Structures*. 2012 Sep 7;21(10):105036. <https://doi.org/10.1088/0964-1726/21/10/105036>
- Hisada Y., Kurimoto M., Mitsumoto S., Suzuoki Y. High-precision Estimation of Dielectric Elastomer Generator Output Considering Leakage Charge. 2022 IEEE 4th International Conference on Dielectrics (ICD). 2022 Jul 3;244–7. <https://doi.org/10.1109/ICD53806.2022.9863507>
- Hoffstadt T, Graf C, Maas J. Optimization of the energy harvesting control for dielectric elastomer generators. *Smart Materials and Structures*. 2013 Aug 27;22(9):094028. <https://doi.org/10.1088/0964-1726/22/9/094028>
- Shian S, Huang J, Zhu S, Clarke DR. Optimizing the electrical energy conversion cycle of dielectric elastomer generators. *Advanced Materials* [Internet]. 2014. <https://doi.org/10.1002/adma.201402291>
- Fan P, Chen H. Optimizing the energy harvesting cycle of a dissipative dielectric elastomer generator for performance improvement. *Polymers*. 2018 Dec 4;10(12):1341.
- Jiang Y, Liu S, Zhong M, Zhang L, Ning N, Tian M. Optimizing energy harvesting performance of cone dielectric elastomer generator based on VHB elastomer. *Nano Energy*. 2020 May;71:104606. <https://doi.org/10.1016/j.nanoen.2020.104606>
- Di K, Bao K, Chen H, Xie X, Tan J, Shao Y, et al. Dielectric elastomer generator for electromechanical energy conversion: A mini review. *Sustainability*. 2021 Sep 2;13(17):9881. <https://doi.org/10.3390/su13179881>
- Skov AL, Yu L. Optimization techniques for improving the performance of silicone-based dielectric elastomers. *Advanced Engineering Materials*. 2017 Nov 27;20(5):1700762. <https://doi.org/10.1002/adem.201700762>
- Yao J, Zang W, Wang Y, Yu B, Jiang Y, Ning N, et al. Largely enhanced service life and energy harvesting stability of dielectric elastomer generator by designing and optimizing compliance of electrodes. *ACS Applied Materials & Interfaces*. 2024 Feb 21;16(9):11595–604. <https://doi.org/10.1021/acsami.3c19158>
- Srivastava AK, Basu S. Exploring the performance of a dielectric elastomer generator through numerical simulations. *Sensors and Actuators A: Physical*. 2021 Mar;319:112401. <https://doi.org/10.1016/j.sna.2020.112401>
- Zhang Y, Ellingford C, Zhang R, Roscow J, Hopkins M, Keogh P, et al. Electrical and mechanical self-healing in high-performance dielectric elastomer actuator materials. *Advanced Functional Materials*. 2019 Feb 21;29(15):1808431. <https://doi.org/10.1002/adfm.201808431>
- Xu Z, Zepeng Lv, Zhang C, Wu K, Morshuis P, Claverie A. Study on Breakdown of Dielectric Elastomer Generators during Energy Harvesting Process. 2022 IEEE 4th International Conference on Dielectrics (ICD). 2024 Jun 30;1–4. <https://doi.org/10.1109/ICD59037.2024.10613228>
- Taine E, Andritsch T, Saeedi IA, Peter. Optimizing energy density in dielectric elastomer generators: a reliability-dependent metric. *Smart Materials and Structures*. 2024 Oct 7; <https://doi.org/10.1088/1361-665X/ad840e>
- Chiba S, Waki M. Innovative power generator using dielectric elastomers (creating the foundations of an environmentally sustainable society). *Sustainable Chemistry and Pharmacy* [Internet]. 2020 Mar 1 [cited 2020 Apr 22];15:100205. <https://doi.org/10.1016/j.scp.2019.100205>

18. Du X, Du L, Li P, Liu X, Han Y, Yu H, et al. A dielectric elastomer and electret hybrid ocean wave power generator with oscillating water column. *Nano Energy* [Internet]. 2023 Jun 15;111:108417. <https://doi.org/10.1016/j.nanoen.2023.108417>
19. Chiba S, Waki M. A marine experiment using dielectric elastomer generators and comparative study with actual measured values and theoretical values. *Archives of Advanced Engineering Science*. 2024 Aug 5; <https://doi.org/10.47852/bonviewAAES42023530>
20. Sikora W. Experimental investigation of a uniaxial dielectric elastomer generator. *Acta Mechanica et Automatica*. 2023 Aug 17;17(4):499–506. <https://doi.org/10.2478/ama-2023-0058>
21. Huang J, Shian S, Suo Z, Clarke DR. Dielectric elastomer generator with equi-biaxial mechanical loading for energy harvesting. *Proceedings of SPIE, the International Society for Optical Engineering/Proceedings of SPIE*. 2013 Apr 9;8687:86870Q86870Q. <https://doi.org/10.1117/12.2009724>
22. Moretti G, Rosset S, Vertechy R, Anderson I, Fontana M. A review of dielectric elastomer generator systems. *Advanced Intelligent Systems*. 2020 Aug 23;2(10):2000125. <https://doi.org/10.1002/aisy.202000125>
23. Rosset S, Anderson IA. Squeezing more juice out of dielectric elastomer generators. *Frontiers in Robotics and AI*. 2022 Feb 11;9. <https://doi.org/10.3389/frobt.2022.825148>
24. Górski F, Denysenko Y, Kuczko W, Żukowska M, Wichniarek R, Zawadzki P, Rybarczyk J. Individualized 3D printed orthopaedic and prosthetic devices using AutoMedPrint technology – Methodologies and Examples. *Advances in Science and Technology – Research Journal*. 2024 Sept 8; 18(6):145–158. <https://doi.org/10.12913/22998624/191548>
25. Rybarczyk J, Górski F, Kuczko W, Wichniarek R, Siwiec S, Vitkovic N, Păcurar R. Mechanical properties of carbon fiber reinforced materials for 3D printing of ankle foot orthoses. *Advances in Science and Technology – Research Journal*. 2024 Jun 20; 18(4):191-215. <https://doi.org/10.12913/22998624/188819>
26. Komorek A, Bakula M, Babel R, Woźniński P, Rośkiewicz M. The influence of 3D printing direction on the mechanical properties of manufactured elements. *Advances in Science and Technology – Research Journal*. 2024 Nov 1; 18(8):86-95. <https://doi.org/10.12913/22998624/193528>
27. Sikora W. Estimating the capacitance of a dielectric elastomer generator using selected measurement methods. 2024 May 22; <https://doi.org/10.1109/ICCC62069.2024.10569981>
28. McKay TG, Rosset S, Anderson IA, Shea H. Dielectric elastomer generators that stack up. *Smart Materials and Structures*. 2014 Dec 5;24(1):015014. <https://dx.doi.org/10.1088/0964-1726/24/1/015014>